Atomic and electronic structures of large and small carbon tori

V. Meunier,* Ph. Lambin, and A. A. Lucas
Département de Physique, Facultés Universitaires Notre-Dame de la Paix, 61 Rue de Bruxelles, B 5000 Namur, Belgium
(Received 3 October 1997; revised manuscript received 27 January 1998)

The stability of large carbon tori is examined within the elasticity theory. Tori of diameter larger than 200 nm obtained by bending a single-wall nanotube and connecting the two ends together are proved to be stable. Molecular mechanics is used for optimizing the structure of a small polygonal torus (C_{1960}) obtained by connecting short portions of (6,6) and (10,0) nanotubes with ten pairs of pentagons and heptagons. The electronic structures of both small and large tori are determined within the framework of a tight-binding Hamiltonian, and their energies are compared. By application of London theory, it is shown that a magnetic field deeply influences the electronic structure of the carbon tori. [S0163-1829(98)02623-X]

I. INTRODUCTION

Recently, circular ropes of single-wall nanotubes have been observed in samples produced by the laser-vaporization technique.[1] In view of the formation mechanism proposed, these objects are most likely made of nanotubes close to the armchair (10,10) configuration, packed together and elastically bent in the form of tori. The curvature radius of these circular ropes was always found to be larger than 150 nm.

Obviously, a nanotube elastically bent and closed upon itself would be unstable upon opening and straightening if the strain energy exceeded the binding energy of the graphitic network. By developing this argument, it is shown below that the critical radius of an elastic torus made of a (10,10) nanotube is around 100 nm, close to the limit found experimentally.

Long before the observation of circular ropes, theoretical constructions of graphitic tori have been proposed in the literature.[2,3] In these hypothetical toroidal objects, positive and negative curvatures were obtained by incorporating an equal number of pentagons and heptagons in the honeycomb network. These defects, which need to be formed during the growth process,[4] allow the relaxation of the strain energy of the structure. As a consequence, tori with curvature radii much smaller than 100 nm can be generated, at least in principle, since there is as yet no clear experimental observations of such small carbon tori.[5] To give an example, the structural properties of a C_{1960} torus obtained by connecting small portions of (6,6) and (10,0) nanotubes are investigated below. It is shown that the strain in this torus remains well below the bond-breaking energy.

Molecular toroids are expected to have interesting diamagnetic properties.[6] Quantum mechanics predicts that the diamagnetic susceptibility of a carbon torus scales like R^2 with the curvature radius, when the magnetic field is perpendicular to the equatorial plane. This law is valid as long as the electron wave functions remain coherent over the length $2\pi R$ of the torus, which means low temperatures as soon as R exceeds several tens of nanometers. Since an armchair nanotube has a metallic conductivity,[7] a torus made from it should also exhibit a Pauli paramagnetism. As shown below, this component of the magnetic susceptibility of the torus can easily be evaluated by a tight-binding Hamiltonian, but it is found to contribute little at room temperature.

The paper is organized as follows. Section II is devoted to elastic tori of large curvature radius. The critical radius is evaluated from known properties of carbon nanotubes. The Pauli susceptibility of tori formed from an armchair single-wall nanotube is also determined there. Polygonal toroidal structures containing pentagon-heptagon pair defects are considered in Sec. III. A short review is given to the carbon toroids already described in the literature. The structural and electronic properties of a C_{1960} torus are then described.

II. ELASTIC TORI

As mentioned in Sec. I, the circular ropes observed by Liu *et al.*[1] are probably bundles of individual (10,10) nanotubes elastically bent around in the form of tori. The nanotubes in a rope are often twisted, but this difficulty is ignored here. Rather, we consider a torus obtained by bending around a single nanotube and connecting its two ends, forming a so-called toroidal polyhex.[8] The stability of such an elastic torus with curvature radius R implies that the C-C bonds are strong enough to accommodate the strain energy $W = \pi IY/R$, where Y is the Young modulus and $I = \pi r^3 t$ is the inertia moment of the cross-sectional array of the nanotube. The latter is considered to be a hollow cylinder with radius r and thickness t, assuming $t \ll r$.

The bond-breaking energy of the nanotube can be estimated to be $E_b = 4\pi\sigma r t$, where σ is the surface tension of graphite perpendicular to the basal planes (4.2 J/m^2).[9] The stability condition of the torus, $W < E_b$, then implies that R be larger than a critical value

$$R_c = \pi r^2 Y/4\sigma, \tag{1}$$

independent of the layer thickness t as long as t remains much smaller than the nanotube radius r. For single-wall tubules, recent calculations yield $Y \approx 1$ TPa,[10] whereas somewhat larger values were determined experimentally on multiwall nanotubes, with an average around 1.8 TPa.[11] With $Y = 1$ TPa, Eq. (1) gives $R_c = 90$ nm for a torus made of a (10,10) nanotube ($r = 0.68$ nm). In view of the uncertainties that remain on both the Young modulus and the surface ten-

sion, this estimation of the critical radius is consistent with the observation that the circular ropes all had curvature radii larger than 150 nm.[1]

In a recent communication, Haddon addressed the question of the diamagnetism of a carbon toroid in relation to its electronic structure.[6] The electronic structure of an elastic torus can easily be sketched from the one of a straight tubule,[8] by applying cyclic boundary conditions along the axial direction in addition to those already applied around the circumference.[12–14] For a torus obtained by bending a section of an *armchair* (L,L) tubule composed of N unit cells along its axis, the highest occupied and lowest unoccupied electronic states have their energies given by $-E_j$ and $+E_j$, respectively, with

$$E_j = |j\gamma_0|\pi/\sqrt{3}N, \quad |j| \ll N, \tag{2}$$

where γ_0 is the $pp\pi$ interaction of the carbon network (≈ -3 eV), and j is a small positive or negative integer such that $N+j$ is a multiple of 3. All the levels j have at least a twofold degeneracy due to the symmetry of the band structure of the nanotube with respect to the Γ point. When $N = M(3)$ (multiple of 3), there is an additional degeneracy due to the $j \leftrightarrow -j$ symmetry in Eq. (2). The levels are regularly spaced by the amount $\Delta E = 3|\gamma_0| d_{nn}/2R$ where $R = N\sqrt{3}d_{nn}/2\pi$ is the curvature radius of the torus, with d_{nn} the C-C distance. When $N \neq M(3)$ (not a multiple of 3), j is no longer equivalent to $-j$, the degeneracy of the levels is lowered as sketched in Fig. 1(a), and a highest occupied molecular orbital (HOMO)–lowest unoccupied molecular orbital (LUMO) gap equal to $2\Delta E/3$ is formed. For $R = 150$ nm, one obtains $\Delta E = 4$ meV.

As shown by Lu for straight nanotubes,[15] a magnetic field may have a strong influence on the electronic structure of the system. The energy levels of the torus are easily obtained within the London theory for a magnetic field perpendicular to the torus. As shown in the Appendix, the energy levels close to the Fermi level move up and down by the amount $\Delta E\,\phi/\phi_0$, where $\phi = \pi R^2 B$ is the flux across the equator and $\phi_0 = h/e$. A consequence is that the HOMO-LUMO gap is a periodic function of ϕ with period ϕ_0 and amplitude ΔE. With a torus of radius of 150 nm, a flux quantum corresponds to 0.06 T.

The energy-level separation of the elastic torus built from an armchair nanotube could be small enough for developing Pauli paramagnetism at room temperature. The paramagnetic susceptibility of the torus at vanishing field deduced from a Zeeman splitting of the energy levels of Fig. 1(a) is

$$\chi_p = 2\mu_0 \frac{\mu_B^2}{k_B T} \sum_j \frac{1}{\cosh^2(E_j/2k_B T)}, \tag{3}$$

where μ_0 is the magnetic permeability of vacuum, and μ_B is the Bohr magneton. This expression is plotted against the temperature in Fig. 1(b) for both the $N = M(3)$ and $N \neq M(3)$ tori. At low T, the discrete structure of the energy levels is apparent: The paramagnetic susceptibility of the torus with N not a multiple of 3 vanishes, whereas the one for $N = M(3)$ follows a Curie law C/T and diverges at 0 K due to the closing of the HOMO-LUMO gap. Therefore, the paramagnetic response of a torus at low temperature makes a

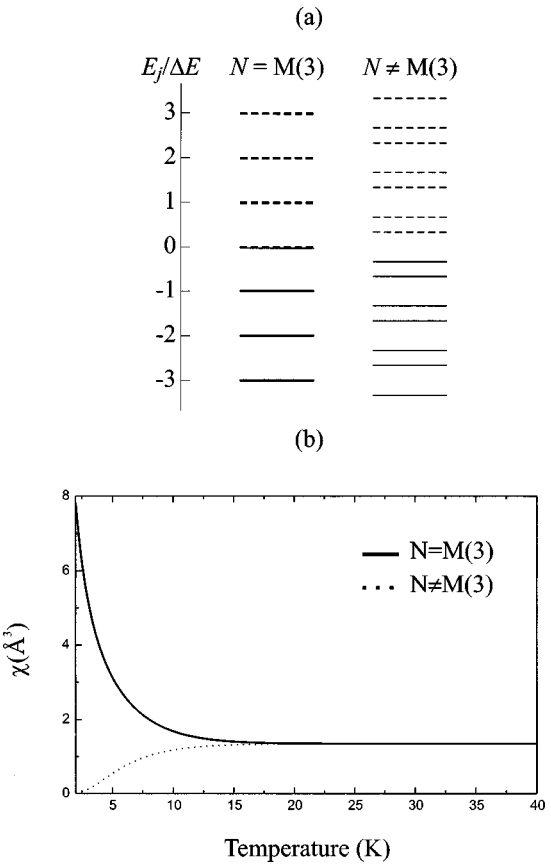

FIG. 1. (a) Highest occupied π-electron states (continuous lines) and the lowest unoccupied π^* states (dashed lines) of a torus obtained by bending around a single-wall armchair tubule composed of $N \gg 1$ unit cells along its axis, and connecting the two ends. (b) Paramagnetic susceptibility of such an elastic torus as a function of the temperature. The energy-level separation used for this calculation was $\Delta E = 4$ meV. Both the electronic structure and the magnetic response of the torus depend on whether N is a multiple of 3 or not.

net differentiation between a ''nonconducting'' torus (finite HOMO-LUMO gap) and a ''conducting'' one (vanishing gap). Above 30 K ($\sim \Delta E/k_B$), both systems have roughly the same susceptibility, independent of the temperature—as it should for a Pauli paramagnetism—and close to the large-T limit of Eq. (3), $8\mu_0\mu_B^2/\Delta E$. Inserting the expression of ΔE and dividing by the number $\mathcal{N}$ of carbon atoms involved, we obtain

$$\lim_{T\to\infty} \chi_p/\mathcal{N} = \mu_0 \mu_B^2 \frac{\sqrt{3}d_{nn}}{\pi^2|\gamma_0|r}, \tag{4}$$

independent of the torus curvature radius R. This is a small contribution, since it accounts for 5×10^{-6} cm^3 per mole C in the case of a (10,10) nanotube, witch is about 20 times smaller than the ring-current diamagnetism of graphite.[16] In spite of this small value, electron-spin resonance measurements indicate a Pauli susceptibility of 0.5×10^{-6} cm^3/mol C for a purified sample of carbon nanotubes.[17] Assuming that one-third of the nanotubes

in that sample were metallic, we obtain $\chi_p/\mathcal{N} \approx 1.5\times10^{-6}$ cm^3/mol C, of the order of the value predicted here for a (10,10) torus.

By comparison, the orbital and diamagnetic susceptibilities of the elastic torus could be much larger and should be highly anisotropic. The largest component is by far the one where the magnetic field is perpendicular to the torus. This component, which is proportional to the square of the curvature radius[6] as long as the phase of the many-body wave function is not destroyed by inelastic scatterings of the electrons, should dominate the magnetization of the elastic torus in the perpendicular geometry. In the parallel geometry, by contrast, the paramagnetic susceptibility of the tori may partly compensate for the diamagnetic component, more especially for the conducting components.

III. POLYGONAL GRAPHITIC TORI

It follows from Sec. II that a torus with a curvature radius smaller than 100 nm demands strong deformations of the structure, leading eventually to the development of kinks.[18] Models of carbon tori have been generated where the kinks are realized at the atomic scale by inserting several pairs of pentagons and heptagons in a graphitic tubular network.[2,3,5,6,19] When a pentagon and heptagon are introduced at diametrically opposed positions in a growing nanotube, the structure makes a sharp bend at an angle of 30°–40°.[20] Such a defect changes the orientation of the graphitic network with respect to the axis. The defect must appear during the growth process,[21] and cannot be the consequence of a plastic deformation because it would require rebonding the whole structure on one side. Junctions between various kinds of nanotubes can be realized by introducing a pentagon-heptagon pair.[2,20,22] By repeating the pentagon-heptagon connections periodically, seamless tori can be generated with curvature radius as small as 1 nm.[23,24]

Several junctions between semiconductor and metallic carbon tubules based on the pentagon-heptagon construction have been generated on the computer, making it possible to investigate the electronic properties of these carbon nanostructures.[25–28] Among these, the (10,0)/(6,6) junction is of special interest. By connecting a semiconductor nanotube to a metallic one, the electronic structure of that junction presents interesting characteristics.[25,28] Moreover, the optimized structure of the (10,0)/(6,6) junction bends at an angle of 36°. It was therefore natural to generate a closed carbon structure by connecting ten such (10,0)/(6,6) patterns. A toroidal molecule incorporating 1960 carbon atoms constructed in this way is shown in Fig. 2. This molecule has D_{5h} symmetry. Its diameter is ~6 nm, which is of the order of the resolution easily achieved with electron microscopes.

Table I is a list of polygonal C toroids already considered in the literature, and which present some similarity with the C_{1960} cluster. The symmetry is most often of orders 5 and 6. In all these toroidal molecules, the number of pentagon-heptagon pairs ranges between 8 and 16. For instance, C_{520} is a construction containing ten pairs of pentagons and heptagons based on the (9,0)/(5,5) junction, where the section (5,5) is reduced to nothing. Similarly, C_{576} is based on the (8,0)/(4,4) junction, where the (8,0) section is very short, and which contains 12 pentagon-heptagon pairs. In C_{1960}, the

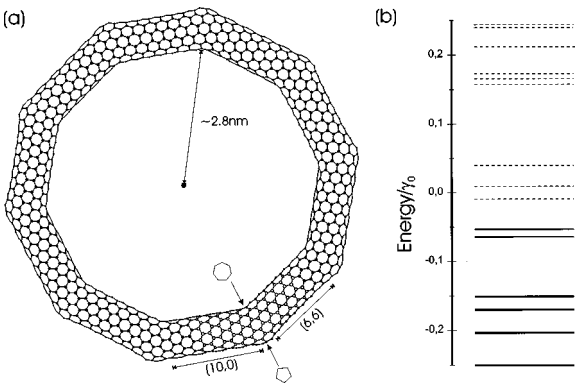

FIG. 2. (a) Optimized structure of the C_{1960} carbon torus with D_{5h} symmetry made from ten (10,0)/(6,6) junctions. (b) Energy levels of the torus near the HOMO-LUMO separation, in units of the $pp\pi$ hopping interaction γ_0. The torus contains ten pentagons and heptagons located at the inner and outer rims of the ring, respectively.

(10,0) and (6,6) sections have similar lengths, which means that the pentagon-heptagon pairs are well separated. In most of the clusters listed in Table I, the pentagons and heptagons are located around the outer and inner equator curves, respectively, of the tori. By contrast, C_{150} contains adjacent pentagons and heptagons on both sides of the equatorial plane.

The atomic structure of C_{1960} shown in Fig. 2(a) was relaxed by application of a simulated-annealing algorithm based on an empirical C-C potential.[29] This molecular-mechanics model is well adapted to fullerenes and related sp^2 carbon networks. It includes two-, three-, and four-body interactions between nearest neighbors, accounting for bond

TABLE I. Graphitic tori containing seven- and five-membered rings.

Torus	Symmetry	Ref.
$C_{120(n^2+m^2+nm)}$, $n=1-4$, $m=0,1$	D_{5d}	a,b,c,d
$C_{80(n^2+m^2+nm)}$, $n=1-4$, $m=0,1$	D_{5d}	e
C_{48k}, $k=4-8$	D_{kd}	e,d
C_{72k}, $k=4-8$	D_{kd}	e,d
C_{90k}, $k=4-8$	D_{kh}	e,f,d
C_{144}	D_{6d}	d
C_{150}	D_{5h}	g
C_{360}	D_{6d}	d
C_{520}	D_{5h}	h
C_{576}	D_{6h}	f,d
C_{600}	D_{6d}	d
C_{1960}	D_{5h}	i

[a]Reference 3.
[b]Reference 35.
[c]Reference 23.
[d]Reference 19.
[e]Reference 36.
[f]Reference 2.
[g]Reference 34.
[h]Reference 5.
[i]This work.

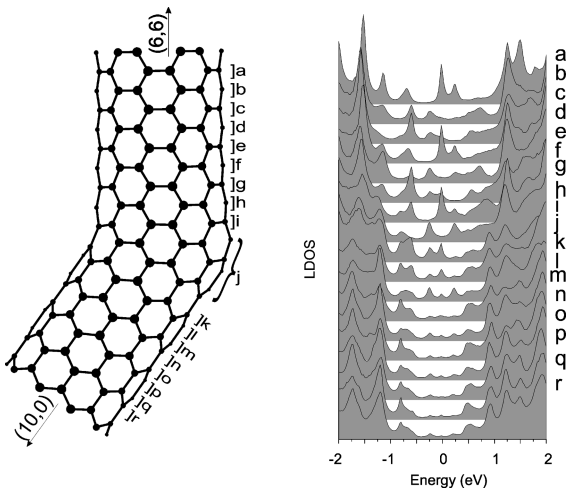

FIG. 3. Local electron density of states in the C_{1960} torus. The curves labeled $a-r$ represent the densities of states averaged over the atoms contained in the belts indicated by the corresponding letters in the irreducible section shown on the left-hand side. An irreducible unit of the torus is indicated by open circles in Fig. 2.

stretching, bending, and torsion, respectively, plus next-nearest-neighbor nonbonding van der Waals interactions. Test calculations performed with the Tersoff-Brenner potential[30] led to essentially the same optimized geometries when applied to single junctions between two nanotube sections.[28] During the optimization process, the symmetry of the torus was preserved.

The electronic structure of C_{1960} was explored with a tight-binding Hamiltonian based on the four C $2s$ and $2p$ valence orbitals. Only first-neighbor interactions were considered in the Slater-Koster description,[31] with parameters fitted to the local-density-approximation band structure of graphite.[32] The C_{1960} torus has a small HOMO-LUMO gap (0.05 eV), still ten times larger than the energy-level separation of the elastic tori considered above. A detailed part of the electronic structure in the region of the HOMO and LUMO states is shown in Fig. 2(b).

Local electronic densities of states (DOS) were computed by the recursion method.[33] This technique leads to a continued-fraction expansion of the density of states as a function of energy. In this work, 150 continued-fraction levels were used with a small imaginary part (0.02 eV) added to the energy to force the convergence. As a result of this procedure, the discrete structure of the electronic levels of the cluster is washed out. In particular, the small HOMO-LUMO gap does not come out in the local DOS of Fig. 3: the peak at the Fermi level E_F (-0.03 eV) is built from both the HOMO and LUMO levels.

Figure 3 shows how the local DOS varies in an irreducible segment of the torus. Clearly, the (6,6) section contains conducting states [all (L,L) armchair tubules are metallic], whereas the (10,0) section is nonconducting [the (10,0) nanotube is a semiconductor with a band gap of 0.70 eV]. The residual states in the gap region of the curves p, q, and r are due to both the 0.02-eV damping factor and tunneling from the metal. Interestingly, the DOS near E_F in the conducting part (curves a–i) does not reproduce the plateau typical of an armchair nanotube. Instead, there are peaks and valleys, which reproduce roughly the same features every other three rings (compare curves a and d, or c and f). This fact was already observed in the case of a single junction between infinitely long (10,0) and (6,6) nanotubes.[25,28] The explanation was that any Bloch state with wave vector k close to the Fermi wave vector k_F is evanescent in the zigzag (10,0) tubule because it falls within the semiconductor band gap. It is therefore reflected back in the conducting section, where it interferes with the incoming state. A standing wave is therefore formed with a spatial period of the local DOS given by $2\pi/2k \approx \pi/k_F = 3\sqrt{3}d_{nn}/2$, that is to say the distance between the a and d belts in Fig. 3. In spite of the finite length of the (10,0) and (6,6) portions of C_{1960}, this standing wave with triple period is reproduced in the torus.

In the C_{1960} torus, the excess of energy with respect to the straight nanotubes deduced from the electronic structure is 28 eV. By increasing the length of the (6,6) and (10,0) sections, larger tori have been generated. Their energy was found increasing slightly with the radius R (32 eV for C_{3280} and 34 eV for C_{4360}). Since the (6,0) and (10,0) sections are only weakly deformed in these tori, the excess energy is essentially due to the pentagon-heptagon defects. The energy of a single such pair connecting infinitely long (10,0) and (6,6) nanotubes is 5.4 eV.[28] This means that the excess energy of the polygonized toroid should approach 54 eV when the length of the (10,0) and (6,6) sections increase to infinity. By contrast, the strain energy of an elastic torus decreases like the reciprocal of its curvature radius R, as emphasized in Sec. II. This definitively favors this kind of torus over the present polygonized version for large R. For small R, however, it is the other way around: the tori containing seven- and five-membered rings have a much lower energy than the ones composed of hexagons only.[34]

IV. CONCLUSION

The structural and electronic properties of both elastic and polygonized carbon tori were examined. Elasticity indicates that the smallest curvature radius R of a defect-free carbon torus made from a single-wall nanotube with radius r around 1.4 nm is close to the value of 150 nm found experimentally. London theory predicts that a magnetic field of 0.1 T, typically, may have a deep influence on the electronic structure of the carbon tori. Tight-binding calculations performed for C_{1960} and larger tori of the same kind show that the introduction of five- and seven-membered rings in the hexagonal network considerably relaxes the bending energy. This makes possible the formation of carbon tori with small curvature radii.

ACKNOWLEDGMENTS

This work was performed under the auspices of the interuniversity research program on Reduced Dimensionality Systems (PAI-IUAP N. P4/10) initiated by the Belgian Federal OSTC. V.M. acknowledges a grant from the Belgian Fund for Industrial and Agricultural Research (FRIA).

APPENDIX: EFFECT OF A MAGNETIC FIELD ON THE ELECTRONIC STRUCTURE OF THE ELASTIC TORUS

We consider a uniform magnetic field B parallel to the torus axis composed of N units of a (L,L) tubule. Assuming

nearest-neighbor hoppings and one π orbital per site, the tight-binding Hamiltonian can be solved analytically, leading to the band structure[14]

$$\varepsilon_n(k_x^m) = \pm \gamma_0 \left\{ 1 + 4 \cos\left(k_x^m \frac{a}{2} \right) \left[\cos\left(k_x^m \frac{a}{2} \right) + \cos\left(\frac{n\pi}{L} \right) \right] \right\}^{1/2}, \tag{A1}$$

where the index n takes any integer value between 0 and $2L-1$, and $a=\sqrt{3}d_{nn}$. Cyclic boundary condition and the application of London theory[15] lead to a discretization of k_x given by

$$k_x^m = \left(m - \frac{\phi}{\phi_0} \right) \frac{2\pi}{Na}. \tag{A2}$$

In this equation, $m=0,1,\ldots,N-1$, $\phi=\mu_0 \pi R^2 H$ and $\phi_0 = e/h$. The levels close to the Fermi energy derive from the bands $n=L$ and come from k_x^m close to $2\pi/3a$. For these levels, one finds

$$\varepsilon_m = \pm \frac{\sqrt{3}\pi\gamma_0}{N} \left| \frac{3m-N}{3} - \frac{\phi}{\phi_0} \right|.$$

From that, we see that the HOMO-LUMO gap is a periodic function of ϕ/ϕ_0 of period 1 which oscillates between 0 and $3d_{nn}\gamma_0/2R$. In Eq. (2) of Sec. II, j was used for $3m-N$, which proves that $N+3j$ is a multiple of 3.

*Electronic address: Vincent.Meunier@fundp.ac.be

[1] J. Liu, H. Dai, J. H. Hafner, D. T. Colbert, R. E. Smalley, S. J. Tans, and C. Dekker, Nature (London) **385**, 780 (1997).
[2] B. I. Dunlap, Phys. Rev. B **46**, 1933 (1992).
[3] S. Itoh, S. Ihara, and J. I. Kitami, Phys. Rev. B **47**, 1703 (1993).
[4] A. Fonseca, K. Hernadi, J. B. Nagy, Ph. Lambin, and A. A. Lucas, Carbon **33**, 1759 (1995).
[5] R. Setton and N. Setton, Carbon **35**, 497 (1997).
[6] R. C. Haddon, Nature (London) **388**, 31 (1997).
[7] Z. Wang, M. Luo, D. Yan, H. Ying, and W. Li, Phys. Rev. B **51**, 13 833 (1995).
[8] E. C. Kirby, R. B. Mallion, and P. Pollak, J. Chem. Soc., Faraday Trans. **89**, 1945 (1993).
[9] M. S. Dresselhaus, G. Dresselhaus, K. Sugihara, I. L. Spain, and H. A. Goldberg, *Graphite Fibers and Filaments* (Springer-Verlag, Berlin, 1988), p. 147.
[10] J. P. Lu, Phys. Rev. Lett. **79**, 1297 (1997).
[11] M. M. J. Treacy, T. W. Ebbesen, and J. M. Gibson, Nature (London) **381**, 678 (1996).
[12] J. W. Mintmire, B. I. Dunlap, and C. T. White, Phys. Rev. Lett. **68**, 631 (1992).
[13] N. Hamada, S. I. Sawada, and A. Oshiyama, Phys. Rev. Lett. **68**, 1579 (1992).
[14] R. Saito, M. Fujita, G. Dresselhaus, and M. S. Dresselhaus, Appl. Phys. Lett. **60**, 2204 (1992).
[15] J. P. Lu, Phys. Rev. Lett. **74**, 1123 (1995).
[16] R. C. Haddon, Nature (London) **378**, 249 (1995).
[17] M. Kosaka, T. W. Ebbesen, H. Hiuara, and K. Tanigaki, Chem. Phys. Lett. **233**, 47 (1995).
[18] B. I. Yakobson, C. J. Brabec, and J. Bernholc, Phys. Rev. Lett. **76**, 2511 (1996).
[19] J. K. Johnson, B. N. Davidson, M. R. Pederson, and J. Q. Broughton, Phys. Rev. B **50**, 17 575 (1994).
[20] B. I. Dunlap, Phys. Rev. B **49**, 5643 (1994); **50**, 8134 (1994).
[21] S. Amelinckx, X. B. Zhang, D. Bernaerts, X. F. Zhang, V. Ivanov, and J. B. Nagy, Science **265**, 635 (1994).
[22] R. Tamura and M. Tsukada, Phys. Rev. B **55**, 4991 (1997).
[23] J. C. Greer, S. Itoh, and S. Ihara, Chem. Phys. Lett. **222**, 621 (1994).
[24] H. Terrones, M. Terrones, and W. K. Hsu, Chem. Soc. Rev. **26**, 341 (1995).
[25] Ph. Lambin, A. Fonseca, J. P. Vigneron, J. B. Nagy, and A. A. Lucas, Chem. Phys. Lett. **245**, 85 (1995); Synth. Met. **77**, 249 (1996).
[26] L. Chico, V. H. Crespi, L. X. Benedict, S. G. Louie, and M. L. Cohen, Phys. Rev. Lett. **76**, 971 (1996).
[27] J. C. Charlier, T. W. Ebbesen, and Ph. Lambin, Phys. Rev. B **53**, 11 108 (1996).
[28] V. Meunier, L. Henrard, and Ph. Lambin, Phys. Rev. B **57**, 2586 (1998).
[29] B. Borštnik and D. Lukman, Fullerene Sci. Technol. **2**, 357 (1994).
[30] D. W. Brenner, Phys. Rev. B **42**, 9458 (1990).
[31] J. C. Slater and G. F. Koster, Phys. Rev. **94**, 1498 (1954).
[32] J. C. Charlier, X. Gonze, and J. P. Michenaud, Phys. Rev. B **43**, 4579 (1991).
[33] R. Haydock, V. Heine, and M. J. Kelly, J. Phys. C **8**, 2591 (1975).
[34] B. Borstnik and D. Lukman, Chem. Phys. Lett. **228**, 31 (1994).
[35] S. Ihara, S. Itoh, and J. Kitakami, Phys. Rev. B **47**, 12 908 (1993).
[36] S. Itoh and S. Ihara, Phys. Rev. B **48**, 8323 (1993).